NOVEL EMI ASSESSMENT METHOD BASED ON STATISTICAL DETECTORS TO PROTECT SENSITIVE DIGITAL RADIO RECEIVERS

Marc Pous [1] [2], Marco Azpúrua [1], Dongsheng Zhao [2], Johannes Wolf [2], Ferran Silva [1]

[1] Universitat Politècnica de Catalunya, Spain, Email: marc.pous@upc.edu
[2] European Space Agency, the Netherlands

ABSTRACT

This paper presents a methodology to assess the degradation performance caused by EMI to digital radio receivers. The procedure developed employs statistical information of the interference and the communication signal to create estimators capable of classifying the disturbances according to metrics like the BER. The estimator is computed using machine learning techniques to relate the changes introduced to the APD diagram with the BER. The methodology has been validated through a laboratory experiment, where a narrowband QPSK system is interfered by additive white gaussian noise with different duty cycle and power level parameters. The validation results show that the estimator operates correctly and overcomes the problematics of relaying on the peak or weighting detectors with fixed resolution bandwidth.

1. INTRODUCTION

Currently, electromagnetic interference (EMI) measurement and assessment methodologies defined at standards can lead to disturbance misjudge. The procedures based on fixed resolution bandwidth and peak detector cannot estimate a communication link performance and might cause over costs and delays in the aerospace industry, especially when the emissions levels are close to the limit lines [1].

This problem is shared with other industries as the methodologies defined to carry out the electromagnetic emissions tests were developed many years ago and have not been adequately updated. In other industries, detectors like the quasi-peak (QP) are still the reference to limit unwanted emissions. Nevertheless, the QP detector was firstly developed in the 1930s to protect narrowband old analog communication systems based on signal-to-noise ratio as the primary figure of merit [2]. On the other hand, industries like the automotive or aerospace do not rely on these types of weighting detectors, using the peak measurement as the reference one. Unfortunately, the use of the peak detector might overestimate the interference, leading the EMC assessment to unreasonable over costs or delays at the production. Otherwise, the use of fixed resolution bandwidth (RBW) different from the communication systems we want to protect implies inaccurate measurements when broadband interferences occur.

When the objective is to determine precisely the performance of an onboard radio receiver or a critic sensor being disturbed, we need more advanced indicators that can be applied in the early stages and do not wait till the integration stage. Hence, it is recommended to employ novelties like statistical detectors and relate their output directly with figures of merit like the bit-error-rate (BER) [3-10].

Several studies demonstrate the relationship of statistical detectors like the Amplitude Probability Distribution (APD) [9] with metrics commonly employed to quantify the performance of the digital radio receivers. In [13], the correlation between APD diagram limit lines or dots has been related to the BER of digital communication systems. Nevertheless, the APD detector is not used in the aerospace industry and is only defined in CISPR 11 for measurements above one gigahertz without a straightforward procedure. Moreover, the latest upgrades on the instrumentation capabilities support the measures based on statistical detectors like the APD [14-16]. Nowadays, different time-domain-based instrumentation captures the statistical interference with excellent accuracy. The real-time receivers or other approaches like the ones presented in [14] can be used to measure the interference with different resolution bandwidths equal to the bandwidth of the radio receivers to be protected.

Nevertheless, a broader study should be performed to establish new limits or the procedure to define them for tailor-made applications. This paper proposes a methodology employing machine learning to define new estimators to determine the degradation produced over a digital radio receiver. The estimators are obtained through the APD diagrams distortion, linking them with the BER. A study case is done for broadband interference when we try to protect a digital radio receiver using a QPSK modulation scheme. The estimators obtained combining communication system simulations and machine learning are validated with in-lab measurements demonstrating that the methodology is suitable to predict the degradation. Furthermore, the estimators found should be easy to implement based on simple decision trees to apply them at the final applications to protect the digital radio devices.

2. METHODOLOGY

The main idea of the assessment methodology is to correlate the changes that EMI produces to a specific communication link at the APD diagram. The APD diagram is defined as the part of the time the measured envelope of an interfering signal exceeds a certain level [13]. The relation between the $APD_R(r)$ and the probability density function of the envelope R is

$$APD_R(r) = 1 - F_R(r) \tag{1}$$

and

$$f_R(r) = \frac{d}{dr} F_R(r) = -\frac{d}{dr} APD_R(r) \tag{2}$$

where $F_R(r)$ is the cumulative distribution function (cdf) and $f_R(r)$ is the probability density function (pdf). Thus, the APD is directly obtained from the expressions shown in (1) and (2), and the more accurate pdf of the disturbance, a better EMC assessment. The APD detector output is represented in APD diagrams, a plot with the percentage of time the ordinate is exceeded on the y-axis and the envelope values on the x-axis.

As mentioned before, the idea of employing the APD is not new [11-12], and it is present in standards like CISPR 16-1-1 and some commercial EMI receivers. Nevertheless, this paper's novelty focuses on the alterations that EMI can produce to the resultant shape of the APD diagram. Each communication signal has an intrinsic APD diagram according to parameters like the modulation scheme, coding, or filtering pulse. Once the interference is introduced within the communication channel, it is added to the valuable signal, changing the statistics of the time-domain signal. Therefore, if the transient has sufficient energy, the alteration of the APD diagram appears. However, it is essential to develop a method capable of quantifying the degradation of the radio receiver according to the changes observed in the APD diagram. The output of the methodology shall give us an objective value related to the main figures of merit used for communication system applications like the BER.

The procedure to estimate the impact on a communication link in terms of BER is the following one. We first simulate a communication link using MATLAB®, generating the signal waveform and channel propagation losses. Then, the time-domain signal is processed to obtain the APD according to equations (1) and (2). This APD diagram is the reference to compare the other APD diagram when the different types of interference are present. Next, we add the disturbances within the channel for the interference cases, demodulate the signal, obtain the BER, and compute the APD simultaneously. Then we compare all the resulting APD diagrams with the free-interference scenario's reference case. The indicators that we obtain are distance measurements between the APD diagrams and the difference between the APD areas.

The last stage is to apply machine learning techniques through feeding the classification learner. The objective is to find out the most accurate indicators to relate the BER with the differences in the APD diagrams. The output of the trained model is an estimator capable of classifying the communication link performance using only the APD diagram as the input. This estimator should be tuned if we want to evaluate different communication systems, as interference may impact the performance differently.

As an example of the changes that interferences can produce to the APD diagram, we analyze a QPSK system interfered by additive white gaussian noise. The received communication signal is partially seen in Fig.1, where the in-phase component of a QPSK using a roll cosine filter is displayed.

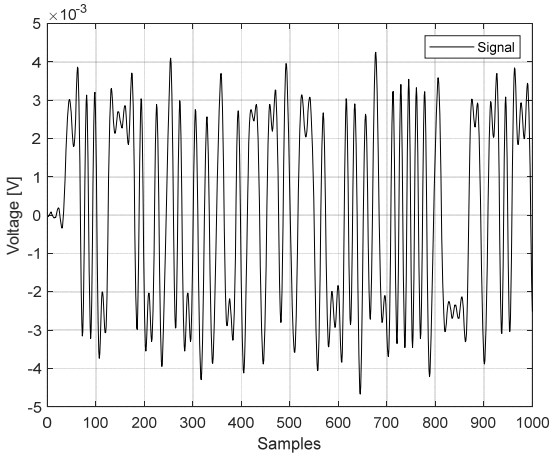

Figure 1. In-phase signal of the QPSK communication system under study.

If we compute the APD diagram of the communication signal, we observe a continuously increasing curve in a smother way (black line in Fig.3). Otherwise, if we generate three different types of additive white gaussian noise (AWGN), we see significant changes in the APD diagram presented in Fig.3. These curves show a heavy-tailed distribution that can be correlated with the duration of the AWGN and its level. Otherwise, in Fig. 2, the time-domain data of the interference and the valuable communication signal is observed for better comprehension. The disturbances that are shown in Fig. 2 are the following ones:

- in blue, the duty cycle of the interference is 0.1, and the level of the interference is close to 0.1 V,
- in red, the duty cycle of the interference is reduced to 0.01 with the same level close to 0.1,
- in green, the duty cycle is 0.1, but the level has

been reduced to values close to 0.4 V.

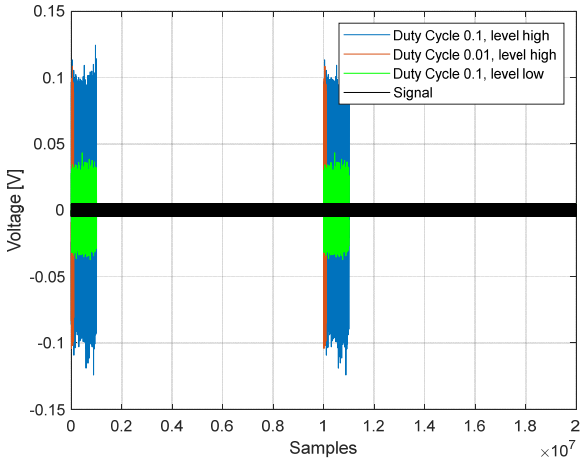

Figure 2. In-phase signal plus interference, varying the duty cycle and the level.

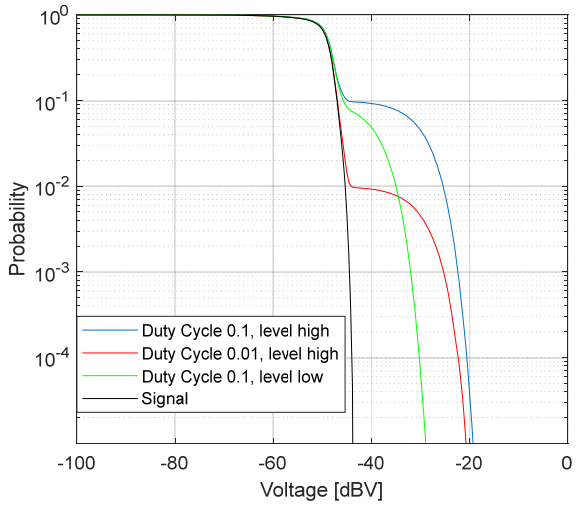

Figure 3. The corresponding APD diagram, where the distortion produced by the interference is observed.

In Fig. 3, we can distinguish the impact of the AWGN duty cycle on the APD curve. As we increase the duty cycle, the straight line of the heavy-tailed distribution becomes more probable, being at higher values. Otherwise, if we focus on the level of the interference, we see that it implies a change at the maximum value recorded by the APD diagram at the x-axis.

Therefore, it is clear that depending on the level of the interference and the duty cycle, the number of bits potentially interfered is different. Nevertheless, by direct observation of the APD diagram, it is complicated to determine the BER, and it confuses more if we consider error correction or coding processing gain. Hence, following the procedure simulating many interference scenarios is necessary to generate a valid estimator that relates the APD diagram and BER. The accurate estimator generation is done in the next section, where we compute APD diagram differences complemented with BER calculations to generate estimators with reduced true/false confusion cases.

3. ESTIMATOR GENERATION

As explained before, to generate an accurate estimator, we should focus on one communication system and an appropriate source of the disturbance. For the study case of this paper, we consider a narrowband QPSK with a 200 kHz bandwidth using a raised cosine filter with a 0.5 rolling factor. On the other hand, we add gated AWGN, varying the interference level and the duty cycle to model suitable interference scenarios. As we analyze a narrowband communication, we can approximate any broadband interference as a flat spectrum noise. Therefore, we can use the gated AWGN model approach commonly employed in communication studies, filtering the interference with the same bandwidth as the communication channel [17].

To generate an accurate estimator, we should simulate many significant cases reaching the margins that the radio link and the interference can have. The disturbance amplitude and the duty cycle have sixteen different values in the study case. The noise power varies between -80 dBm and +10 dBm, and the duty cycle is modified from 0.01 % to 50 %, making a total of 256 cases to generate the estimator. Apart from computing the reference APD diagram and the APD for each interference case, we obtain the BER and the Error Vector Magnitude (EVM). We store the BER and EVM as reference values, and we compute different indicators that can be useful for obtaining a simple and accurate estimator. In this regard, we calculate unique value distances between the different APD curves and the reference one, including the Euclidean, Chebyshev, or Hamming between others. On the other hand, we compute the APD's diagram area, comparing the reference case with the 256 interference cases. All this data is used to feed the machine learning to obtain the suitable estimator that should determine the BER focusing on the differences obtained at the APD diagram.

According to the BER, the estimator is designed to distinguish between three different error categories. We consider the three following categories:

- Class A is defined for a BER higher than 10 %,
- Class B with a BER between or equal to 10% and 1%,
- Class C with a BER lower than 1%.

After evaluating the combination of thirty-five possible

indicators, the resultant estimator is a coarse tree with three decision levels. The estimator only employs the APD area difference and the maximum level of the interference. With this simple estimator, we can predict correctly the 84.5 % of the total cases simulated, with some mismatch at the frontier cases. Otherwise, if we create an estimator using the accepted EVM metrics instead of using the estimator based on the APD, we achieve an accuracy of 70.7 %. Hence, the accuracy of estimating interference scenarios with the new methodology is comparable and even higher than using the EVM. It is essential to mention that the EVM is a reference for communication systems evaluation performance, being widely accepted to characterize communication links performance. Moreover, specific instrumentation is designed to obtain the EVM, but this high-end instrumentation requires to have the communication signal as a principal difference of our approximation.

Nevertheless, we need to validate if the approach of the machine learning estimator based on the APD diagram differences performs appropriately in real interference scenarios. Therefore, an experiment is carried out at the EMC laboratory to evaluate the validity.

4. VALIDATION MEASUREMENTS

To validate the estimators' methodology, we create a communication link using two antennas working at 433 MHz. The experiment is carried out inside an anechoic chamber to avoid other sources of interference and undesired propagation phenomena like multipath. Otherwise, these phenomena can degrade the communication signal and increase the BER. In our experiment, the communication link is disturbed by the EM field produced by a third antenna propagating a gated WGN disturbance into the communication channel.

The communication signal and the AWGN have been generated using the same functions employed before to obtain the estimators. The signal and the interference data are transferred to a Universal Software Radio Peripheral (USRP) by National Instruments model B210. The USRP outputs are connected to two Schwarzbeck UBAA 9115 biconical antennas inside the anechoic chamber. These two antennas are placed at one side of the chamber, one is generating the EM field for the valid signal and the other is creating the AWGN interference. At four meters, we place another equal antenna to receive the signal plus the interference, as shown in Fig. 4. This antenna is connected to the R&S ESW EMI test receiver to obtain the communication signal plus the disturbance. Although this receiver offers us the possibility to compute the APD directly, we do not use this function because the RBW to perform the measurement is limited to predefined values different from the 200 kHz bandwidth of the communication system.

Moreover, as we are interfering with a broadband disturbance, changes on the RBW significantly impact the APD diagram [8]. Alternatively, we obtain the in-phase and quadrature data available at the receiver. Afterward, the data is downloaded to a laptop, where we first filter the 200 kHz channel bandwidth. Then, the filtered data are processed in MATLAB® to obtain the BER, compute the APD diagrams, and derive the output of the previously created estimator.

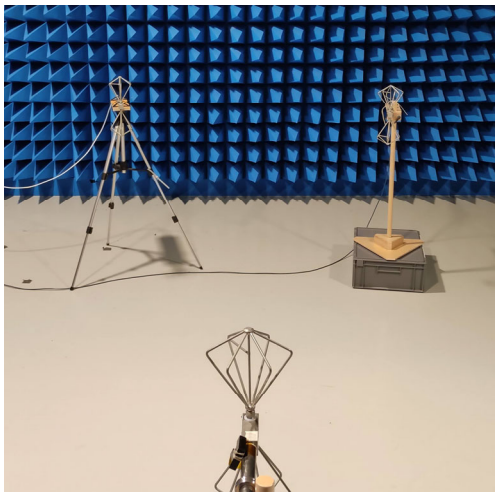

Figure 4. Picture of the measurement setup for validation purposes.

In Fig. 5, we can observe the resulting APD diagram for the useful signal when there is no interference present (in black) and six cases of interference diagrams.

The six different disturbance cases modify the duty cycle and the amplitude of the AWGN. The duty cycle has three different values 0.2, 0.02, and 0.002, as it can be found in Table 1. On the other hand, the amplitude of the generated AWGN is modified by changing the gain parameter of the USRP between 70 dB, 65 dB, and 60 dB. Nevertheless, as the noise generated is random, and we have the 200 kHz filter contribution, the amplitudes of the APD diagram differs from the 5 dB steps. We are using the same time-domain data to compute the APD diagram and the BER for validation purposes. Therefore, we can correlate if the estimator generated beforehand is capable of predicting the performance of the radio receiver for the six cases of interference.

In Fig. 5, it is observed that the several interferences produced a visible change at the APD diagram if we compare them to the reference. Heavy-tailed distributions are produced, modifying the area of the APD diagram with different values of the maximum

level of interference and curves fitting different probabilities. However, direct observation of the graph is complicated to accurately define the influence of the different disturbances on the BER. To relate them, we have to apply the estimator obtained in Section 4 to classify the disturbances accordingly to the BER interval defined before. The BER has been stored for validation purposes and is the reference to check if the estimator can predict the error class or fails.

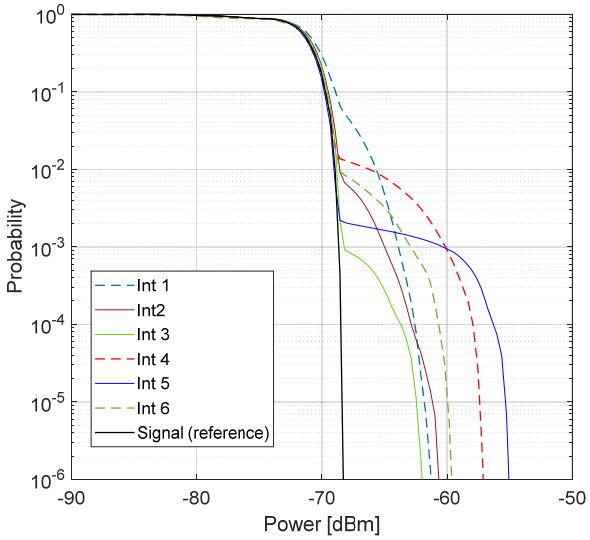

Figure 5. APD results for the different types of interference.

Table 1. Comparison between the estimator classification and the BER measured for the different types of interference.

Interference	Duty Cycle	Peak level measured (dBm)	BER measured	Expected BER Class using the estimator
Int 1	0.2	-61.34	1.09 %	B (10 % ≥ BER ≥ 1 %)
Int 2	0.02	-60.58	0.42 %	C (BER < 1 %)
Int 3	0.002	-61.72	0.09 %	C (BER < 1 %)
Int 4	0.02	-57.1	34.54 %	A (BER > 10 %)
Int 5	0.002	-54.88	21.43 %	A (BER > 10 %)
Int 6	0.02	-59.44	4.17 %	B (10 % ≥ BER ≥ 1 %)

In Table 1, it is observable that the estimator output classification matches all the studied cases. Hence, we can predict the performance of the digital radio receiver when AWGN with different parameters is added to the communication channel. Furthermore, we can identify the worst cases that produce errors higher than 10 % (Int 4 and Int 5), the intermediate cases, where the BER is between 10 % and 1 % (Int 1 and Int 6), and the meaningless interferences that cause an error lower than 1 % (Int 2 and Int 3).

It is essential to highlight that the currently accepted methodology for the aerospace sector is based on peak measurement. Nevertheless, as it is shown in Table 1, the disturbance with the highest peak level is not causing the largest BER, and on the other hand, the disturbances with a peak level of -60 dBm ± 3 dB cause all the different types of errors defined. Therefore, we should move from the peak or weighting detectors to statistical measurements to unequivocally determine the distortion produced over a digital radio receiver.

5. CONCLUSIONS

The methodology explained in this paper shows that it is feasible to create estimators capable of evaluating properly EMI interfering digital radio receivers. The estimator obtained employing machine learning uses the APD diagrams as the primary input, and it is capable of accurately classifying the different types of disturbances. The work presented in this paper is focused on AWGN and a narrowband QPSK system. However, the methodology can be extended to other communication links and another type of interference. Furthermore, this methodology brings us the opportunity to employ statistical detectors and provide better outputs to assess EMI in comparison with traditional peak detector measurements. Moreover, it can overcome the problematics of using weighting detectors with fixed resolution bandwidths and relate the output with figures of merit like the BER.

As the estimator is tailor-made for each radio device to protect, it can be challenging to standardize them. However, its usage can be implemented quickly to protect critic radio links as specific applications for the aerospace industry. Finally, it is essential to continue studying these estimators based on the APD, considering other types of interference like broadband pulses or chirp. This study is even more interesting for broadband radio links as the AWGN approximation can be compromised.

6. ACKNOWLEDGMENT

The project on which these results are based has received funding from the European Union's Horizon 2020 research and innovation programme under Marie Skłodowska-Curie grant agreement No. 801342 (TecniospringINDUSTRY) and the Government of Catalonia's Agency for Business Competitiveness (ACCIÓ).
This work was supported by the Spanish "Agencia Estatal de Investigación" under project PID2019-106120RB-C31/AEI/10.13039/501100011033.

7. REFERENCES

1. M. Pous, M. A. Azpúrua and F. Silva, "Improved Electromagnetic Compatibility Standards for the Interconnected Wireless World," *2019*

International Symposium on Electromagnetic Compatibility - EMC EUROPE, 2019, pp. 1055-1060.

2. G. A. Jackson, "The early history of radio interference," *in Electronic and Radio Engineers, Journal of the Institution of*, vol. 57, no. 6, pp. 244-250, November-December 1987.

3. Y. Matsumoto, "On the Relation Between the Amplitude Probability Distribution of Noise and Bit Error Probability," *IEEE Transactions on Electromagnetic Compatibility*, vol.49, no.4, pp.940,941, Nov. 2007

4. M. Pous, M. A. Azpúrua and F. Silva, "Measurement and Evaluation Techniques to Estimate the Degradation Produced by the Radiated Transients Interference to the GSM System," *in IEEE Transactions on Electromagnetic Compatibility*, vol. 57, no. 6, pp. 1382-1390, Dec. 2015.

5. Wu, I., et al., "Characteristics of Radiation Noise from an LED Lamp and Its Effect on the BER Performance of an OFDM System for DTTB," *IEEE Transactions on Electromagnetic Compatibility*, vol.56, no.1, pp.132-142, Feb 2014.

6. S. Dudoyer, et al., "Classification of Transient EM Noises Depending on their Effect on the Quality of GSM-R Reception," *IEEE Transactions on Electromagnetic Compatibility*, vol.55, no.5, pp.867,874, Oct. 2013.

7. P. F. Stenumgaard, "Using the root-mean-square detector for weighting of disturbances according to its effect on digital communication services," *in IEEE Transactions on Electromagnetic Compatibility*, vol. 42, no. 4, pp. 368-375, Nov 2000.

8. M. Pous and F. Silva, "Full-Spectrum APD Measurement of Transient Interferences in Time Domain," *in IEEE Transactions on Electromagnetic Compatibility*, vol. 56, no. 6, pp. 1352-1360, 2014.

9. M. Pous and F. Silva, "Prediction of the impact of transient disturbances in real-time digital wireless communication systems," *in IEEE Electromagnetic Compatibility Magazine*, vol. 3, no. 3, pp. 76-83, 3rd Quarter 2014.

10. M. Stecher, "A weighting detector for the effect of interference on digital radiocommunication services," *Electromagnetic Compatibility, 2003. EMC '03. 2003 IEEE International Symposium on*, Istanbul, 2003, pp. 449-452 Vol.1.

11. A.D. Spaulding and R.T Disney. Man-Made Noise: Estimates for Business, Residential and Rural Areas. Technical report, Office of Telecommunications, 1976.

12. R. A. Shepherd, "Measurements of amplitude probability distributions and power of automobile ignition noise at HF," *in IEEE Transactions on Vehicular Technology*, vol. 23, no. 3, pp. 72-83, Aug. 1974.

13. Wiklundh, "Relation between the amplitude probability distribution of an interfering signal and its impact on digital radio receivers", *IEEE Trans. on EMC*, pp. 537-544, Aug. 2006.

14. H. H. Slim, C. Hoffmann, S. Braun, and P. Russer, "A novel multichannel amplitude probability distribution for a time-domain EMI measurement system according to CISPR 16-1-1," *10th International Symposium on Electromagnetic Compatibility, York*, 2011, pp. 22-25.

15. M. A. Azpúrua, M. Pous and F. Silva, "Statistical Evaluation of Measurement Accuracy in Full Time-Domain EMI Measurement Systems," *2020 International Symposium on Electromagnetic Compatibility - EMC EUROPE, 2020*, pp. 1-6.

16. M. A. Azpúrua, M. Pous and F. Silva, "Specifying the Waveforms for the Calibration of CISPR 16-1-1 Measuring Receivers," *in IEEE Transactions on Electromagnetic Compatibility*, vol. 62, no. 3, pp. 654-662, June 2020.

17. D. Middleton, "Canonical and quasi-canonical probability models of Class A interference," *IEEE Transactions on Electromagnetic Compatibility*, vol. EMC-25, no. 2, pp. 76 103, May 1983.